Covalently Trapped Triarylamine-Based Supramolecular Polymers

Ting Liang, Dominique Collin, Melodie Galerne, Gad Fuks, Andreas Vargas Jentzsch, Mounir Maaloum, Alain Carvalho, Nicolas Giuseppone, Emilie Moulin

Covalently trapped triarylamine-based supramolecular polymers

Ting Liang,[a] Dominique Collin,[b] Melodie Galerne,[a] Gad Fuks,[a] Andreas Vargas Jentzsch,[a] Mounir Maaloum,[a] Alain Carvalho,[b] Nicolas Giuseppone*[a] and Emilie Moulin*[a]

[a] Dr. T. Liang, M. Galerne, Dr. G. Fuks, Dr. A. Vargas Jentzsch, Prof. Dr. M. Maaloum, Prof. Dr. N. Giuseppone, Dr. E. Moulin
SAMS Research Group, Institut Charles Sadron, CNRS - UPR 22, University of Strasbourg, 23 rue du Loess, BP 84047, 67034 Strasbourg Cedex 2, France
E-mail: giuseppone@unistra.fr; emoulin@unistra.fr

[b] Dr. D. Collin, A. Carvalho
Institut Charles Sadron, CNRS - UPR 22, 23 rue du Loess, BP 84047, 67034 Strasbourg Cedex 2, France

Abstract: *C*$_3$-symmetric triarylamine trisamides (TATAs), decorated with three norbornene end groups, undergo supramolecular polymerization and further gelation by π-π stacking and hydrogen-bonding of their TATA cores. By using subsequent ring opening metathesis polymerization, these physical gels are permanently crosslinked into chemical gels. Detailed comparisons of the supramolecular stacks in solution, in the physical gel, and in the chemical gel states are performed by optical spectroscopies, electronic spectroscopies, atomic force microscopy, electronic paramagnetic resonance spectroscopy, X-ray scattering, electronic transport measurements, and rheology. The results presented here clearly evidence that the core structure of the functional supramolecular polymers can be precisely retained during the covalent capture whereas the mechanical properties of the gels are concomitantly improved, with an increase of their storage modulus by two orders of magnitude.

Introduction

Supramolecular polymers based on triarylamine motifs represent a new and attractive class of functional materials.[1] Their local structure rests on the collinear arrangement of their nitrogen center which is maintained by π–π-stacking and supplementary hydrogen bond interactions (implemented for instance by the addition of amide functions at the periphery of the triarylamine core). These primary structures usually show cooperative mechanisms of polymerization, and their columnar primary stacks can be further self-assembled in various superstructures including bundles of fibers and gels.[2–8] Because of their supramolecular packing, and because triarylamines are prone to be (photo)oxidized, these fibers can be doped to access hole transporting nanowires and conducting materials with peculiar electronic and optical properties.[5,9–11] Still, the supramolecular polymerization of triarylamines usually leads to soft nano-objects and materials which would benefit of being mechanically strengthened. In the present study, we have explored the possibility to chemically and permanently cross-link supramolecular polymers of triarylamines in order to reinforce their mechanical properties and, at the same time, to probe if their main intrinsic structures and functionalities would be retained. Several chemical methods have already been described and reviewed[12] in the literature to cross-link low molecular weight gelators, including photopolymerization of methacrylate[13] and diacetylene,[14] Cu-catalysed 1,3-dipolar cycloaddition,[15] triethoxysilane hydrolysis-condensation,[16] and cross metathesis.[17–19] Another very attractive chemical tool is the ring opening metathesis polymerization reaction (ROMP) of norbornene derivatives.[20] This was used in particular to permanently cross-link conducting supramolecular assemblies made of stacked hexabenzocoronene (HBC) in solution.[21,22] ROMP was also successfully used for the crosslinking of other stacked structures in solution such as perylene, oligothiophene,[23] and *C*$_3$-symmetric trisubstituted benzene.[24] However, it should be noted that, to the best of our knowledge, ROMP has not yet been employed to freeze supramolecular structures in the gel state. Here, we show that ROMP can be an effective tool to generate covalent cross-links in a physical gel while retaining a number of its structural and functional properties.

Results and Discussion

The following experimental study is based on the *C*$_3$-symmetric molecule **1** which has *i*) a typical triarylamine trisamide (TATA) core to undergo supramolecular polymerization, and *ii*) three norbornene end groups on the side chains to trap the resulting self-assembly by covalent capture (Scheme 1).

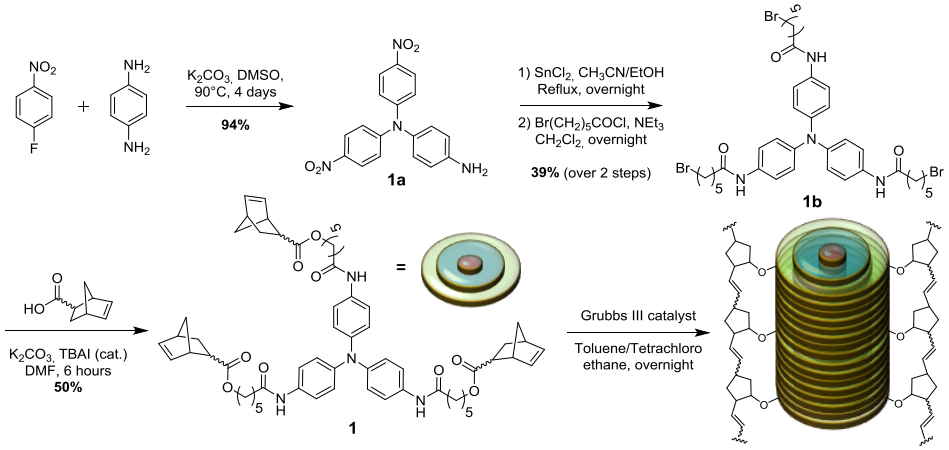

Scheme 1. Synthetic pathway used to access C_3-symmetric triarylamine trisamide (TATA) **1** decorated with norbornene end groups and its polymerization using ROMP with Grubbs III catalyst.

The synthesis of **1** was performed in four steps from commercially available compounds as follows. Compound **1a** was first obtained following a typical aromatic nucleophilic substitution,[5] and subsequently reduced using tin chloride in a 1:1 mixture of acetonitrile and ethanol at reflux. The corresponding tris-amine was then acetylated with 6-bromohexanoyl chloride to give compound **1b** in reasonable yields. Finally, nucleophilic substitution of the terminal bromine with 5-norbonene-2-carboxylic acid provided the expected TATA **1** as a mixture of endo/exo (2:1) compounds (see experimental section and supporting information (SI) for further details).

The spectroscopic properties of **1** were first studied in chloroform solutions at a concentration of 0.1 mM. Upon light irradiation (halogen lamp, 10 $W.cm^{-2}$), we observed a series of typical features (Figure 1a-c) associated with the stacking of TATA molecules which include: a) disappearance of the ^1H NMR resonance signals corresponding to the triarylamine core[25] (Figure S1); b) appearance of a NIR absorption band at ~1130 nm (for shorter times of irradiation and corresponding to the presence of intermolecular through-space radical cation charge-transfer between stacked triarylamine cores), followed by the appearance of an absorption band at ~830 nm (for longer times of irradiation and corresponding to more localized triarylammonium radical cations);[5] c) appearance of a typical three-line pattern on the EPR spectra after irradiation confirming the presence of an unpaired electron on the triarylamine core;[5] and d) disappearance of the fluorescence around 500 nm after short irradiation times which indicates the presence of supramolecular polarons quenching the aggregation induced emission of the stacked TATA molecules, as already described previously in the literature.[5] We also probed the conductivity (*I*/*V* curve) of photo-doped compound **1** at a concentration of 17 mM. By using commercially available ITO electrodes separated by a length gap of 4 µm, the observed ohmic behavior was found very similar to the one recorded for a reference TATA molecule with simple C12 alkyl chains and no norbornenes (Figure 1d).[5]

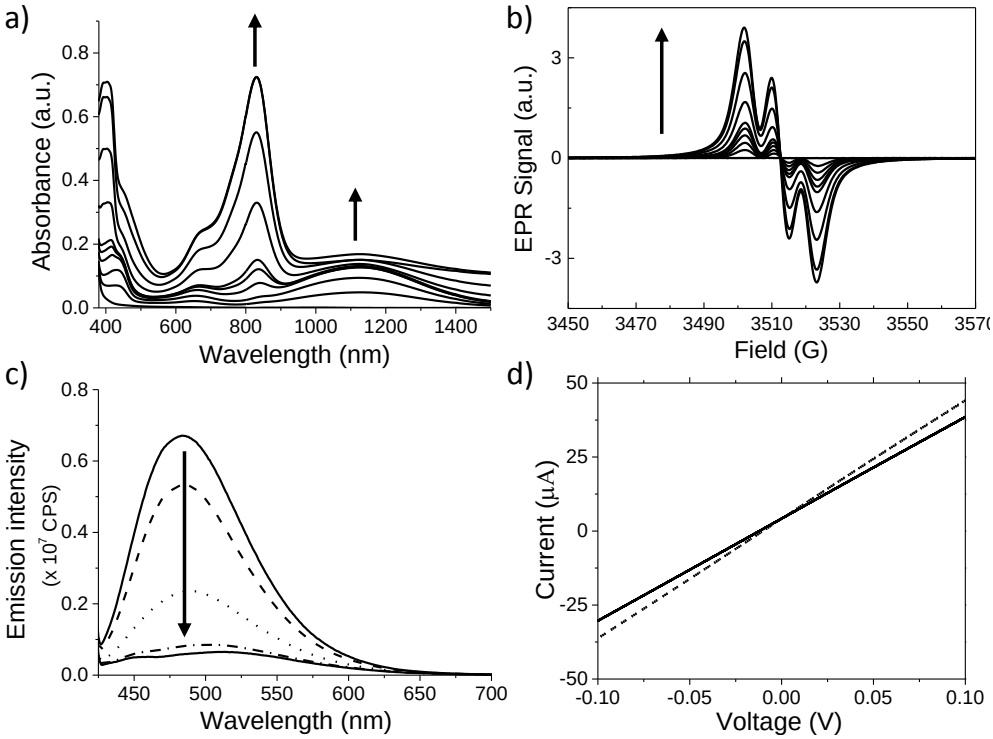

Figure 1. a) UV-Vis-NIR spectra of a 10^{-4} M solution of compound **1** in chloroform upon sequential light irradiation (from 0 to 60 minutes), the arrows indicate the evolution of the absorption bands at 832 and 1129 nm with increasing times of irradiation; b) EPR spectra of a 10^{-4} M solution of compound **1** in chloroform upon sequential light irradiation (from 0 to 60 minutes), the arrow indicates the evolution of the EPR spectra with increasing times of irradiation; c) Evolution of the fluorescence spectra corresponding to a 10^{-4} M solution of compound **1** in chloroform upon sequential light irradiation (from 0 to 5 minutes), the arrow indicates the evolution of the emission with increasing times of irradiation; d) *I-V* curves recorded after a light irradiation of 50 seconds of TATA-C12 (dashed line)[5] and compound **1** (plain line) at a concentration of 17 mM in pure tetrachloroethane.

We then studied the gelation properties of compound **1** in toluene, a solvent which strengthens the supramolecular polymerization of TATA compared to chlorinated solvents, and which facilitates the mechanical studies of the corresponding gels. After a heating/cooling process, compound **1** forms self-supporting gels in toluene for concentrations higher than ~8 mM (~7.9 mg/mL) (Figure S2). TEM and AFM imaging experiments from 1 mM toluene solutions (below the onset gelation concentration) also demonstrate the formation of micrometric long fibers with sections presenting a slight ribbon-like character, of about ~100 nm in width and ~20 nm in thickness (Figures 2a-b and S5a-b). The internal organization along the main axis of these fibers was shown to be made of single columns of TATA with a diameter of ~2.0 nm (Figure S5c-d). Infrared spectroscopy was then used to understand the local organization of these self-assembled structures at the same concentration of 1 mM (Figure S3a). The presence of well-defined bands at ~3290 and 1650 cm^{-1} are characteristic of hydrogen-bonded N-H and C=O stretching bands respectively. In addition, their high symmetry suggests a three-fold helical arrangement of the molecules with intermolecular hydrogen bonds between adjacent TATA cores, as previously described for such compounds in the literature.[5,8,26,27] Above the onset gelation concentration, the morphology of the individual fibers in the physical gel (15 mM in toluene; hereafter referred to as sample A) was found to be similar to those probed from solutions, as observed for instance by SEM imaging of the corresponding aerogel (Figure 2c).

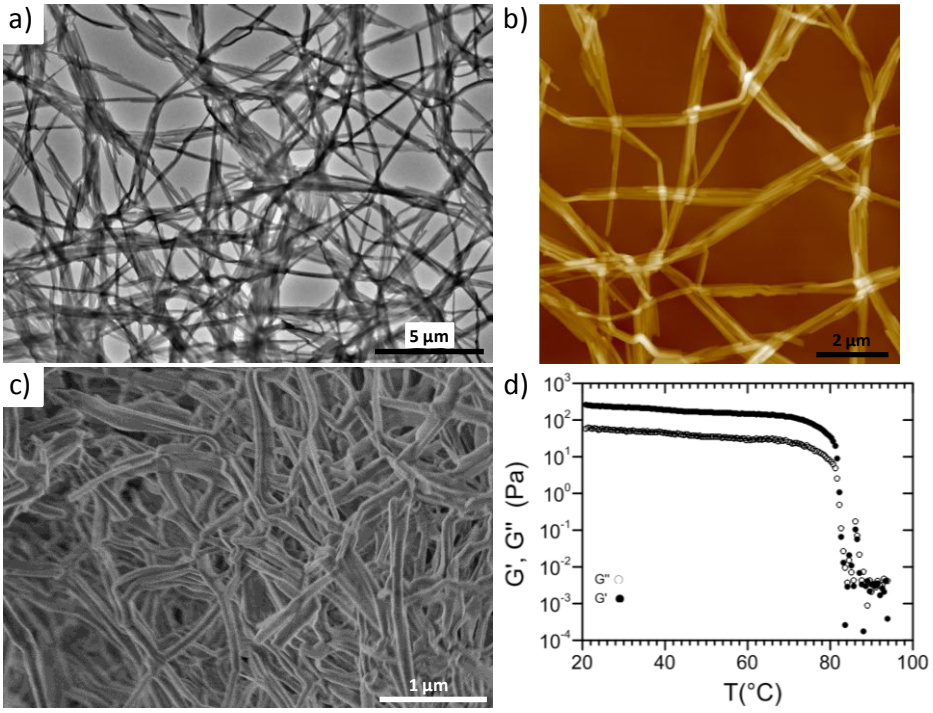

Figure 2. a-b) TEM (a) and AFM (b) images of a 1 mM solution of compound **1** in toluene; c) SEM image of the aerogel obtained from the cooling to room temperature of a 15 mM solution of compound **1** in hot toluene; d) Variation of the storage G' and loss G'' moduli as a function of temperature for a physical gel made of compound **1** in pure toluene (sample A, [**1**] = 15 mM).

We then examined the mechanical properties of that gel (Sample A) in pure toluene (Figure 2d). At room temperature, the variation of the complex shear modulus G* with frequency shows that the storage modulus G' is always greater than the loss modulus G'' and that both moduli remain quasi-constant over the whole range of frequencies studied (0.05 to 10 Hz, Figure S4a). This G* behavior, of the viscoelastic type, is characteristic of a physical gel in the hydrodynamic regime. At 20 °C and for a frequency of 1 Hz, the shear modulus rigidity of the gel was found ~ 260 Pa. To determine the sol to gel temperature transition (T_{gel}), the variation of the complex shear modulus was followed at a fixed frequency of 1 Hz from 95 °C to 20 °C and with an applied cooling rate of -1 $K.min^{-1}$. From high to low temperature, G* values change progressively in agreement with a transition from a liquid to a gel, and T_{gel} (as defined by the intercept between G' and G'') was estimated to occur at around 82 °C. However, our instrumental set-up does not allow a heating of the sample above T_{gel} for long enough time in order to remove any possible aggregates in the liquid phase because of partial solvent evaporation. This constraint was overcome by decreasing the sol-gel transition temperature using a mixture of solvents. In particular, we examined the possibility of adding a chlorinated co-solvent because it would concomitantly allow for a light-induced oxidation process of the TATA molecules. We found that compound **1** at 15 mM in a solvent mixture made of toluene (90%) and tetrachloroethane (10%) (named hereafter as sample B) shows a T_{gel} around 63 °C (Figure 3a). Interestingly, this change in solvent almost did not affect the shear modulus rigidity of the gel (G' = 302 Pa for a frequency of 1 Hz and at 20 °C). Similarly to physical gels formed in pure toluene, SEM imaging of the aerogel made of sample B suggested the presence of dense networks of ribbon-like bundled fibers with lengths of several microns and widths of about 100 nm (Figure 3b-c). Considering that, upon light irradiation, chlorinated solvents can be used as an electron acceptor to trigger the oxidation of the fibers made of TATA molecules,[5] we subsequently studied the influence of this photo-doping process on the spectroscopic, conducting, and rheological properties of sample B. We then compared the results obtained in the gel state using the toluene/tetrachloroethane mixture, with what can be obtained in pure chlorinated solvents. Spectroscopically, a continuous increase of a NIR absorption band at ~1106 nm was observed during the first 20 minutes of irradiation, and then remained constant for longer irradiation times (Figure 3d). Meanwhile, the absorption band at 818 nm starts to increase for irradiation times longer than 20 minutes but without reaching high intensities. This observation indicates that mainly delocalized radicals in the form of polarons within stacks of TATA units were formed. This interpretation is reinforced by EPR experiments in which the hyperfine splitting made of a three line pattern is clearly superimposed with a central one-line pattern characteristic of the presence of fully delocalized radicals with no energetic barrier to charge transfer (Figure 3e as compared with Figure 1b).[5,28] We also probed the conductivity of the physical gel upon light irradiation using commercially available ITO electrodes with a gap of 4 □m (Figure 3f). While sample B shows low conductivity in the neutral state (i.e. before light irradiation), photo-oxidation induces a transition to a conducting state with a characteristic ohmic behavior. Finally, from a mechanical point of view, light irradiation of sample B induces a slight decrease of T_{gel} from 63 °C to 61 °C for irradiation times longer than 15 min (see insert in Figure 3a).

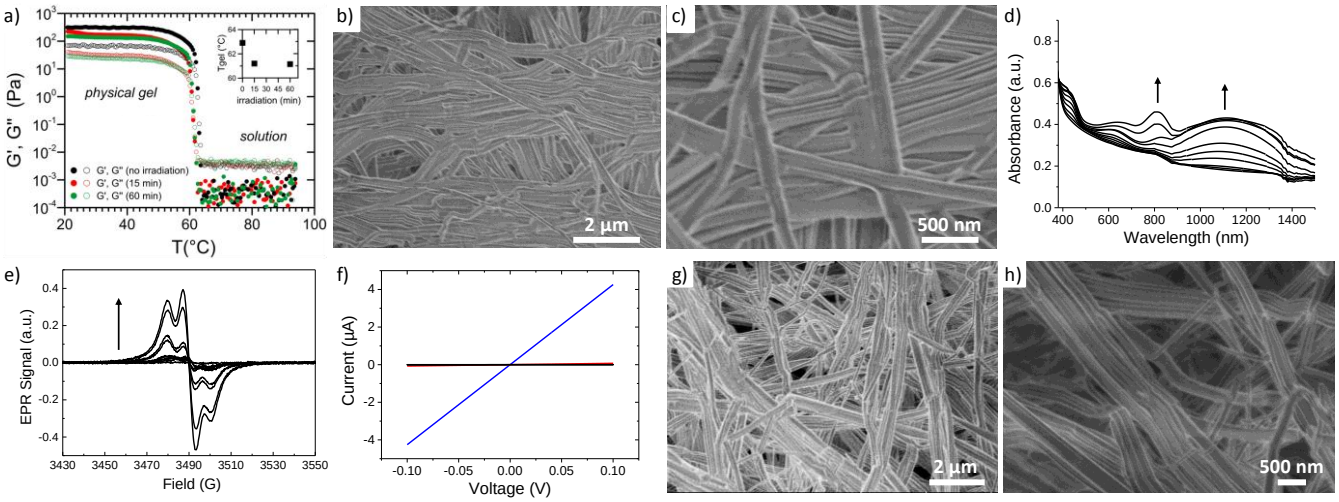

Figure 3. a) Variation with temperature of the real (G') and imaginary (G") parts of the complex shear modulus at a frequency of 1 Hz for the physical gel made of compound **1** in a toluene/10% tetrachloroethane mixture (sample B, [**1**] = 15 mM) without light irradiation (black), and with 15 minutes (red) and 60 minutes (green) light irradiation. The applied cooling rate was -1K/min. The insert shows the shift of T_{gel} induced by light irradiation; b-c) SEM images of the aerogel made of compound **1** in a toluene/10% tetrachloroethane mixture (15 mM, sample B) before light irradiation; d) UV-Vis-NIR spectra of the physical gel made of compound **1** in a toluene/10% tetrachloroethane mixture (15 mM, sample B) upon sequential light irradiation (from 0 to 60 minutes), the arrows indicate the evolution of the absorption bands at 818 and 1106 nm upon irradiation; e) EPR spectra of the physical gel made of compound **1** in a toluene/10% tetrachloroethane mixture (15 mM, sample B) upon sequential light irradiation (from 0 to 60 minutes), the arrow indicates the evolution of the EPR spectra with increasing irradiation times; f) *I-V* curves recorded before irradiation (black) and after 15 (red) and 60 (blue) minutes light irradiation for a physical gel made of compound **1** in a toluene/10% tetrachloroethane mixture (15 mM, sample B); g-h) SEM images of the aerogel made of compound **1** in a toluene/10% tetrachloroethane mixture (15 mM, sample B) after 60 minutes light irradiation.

Following the same trend, we also measured a slight decrease of both G' and G'' with light irradiation (for a frequency of 1 Hz and at 20 °C, G' = 226 and 152 Pa for 15 min and 60 min of irradiation time respectively, Figures 3a and S4b). As shown by the phase measurements (see insert Figure S4b), the decrease in G' and G'' for the gel does not induce a change in the G'/G'' ratio, which is found constant with frequency and roughly independent of the irradiation time. As a result, all the measurements in this frequency range belong to the hydrodynamic regime, regardless of light irradiation. The relative integrity of the supramolecular polymers and gel structures therefrom upon photodoping were confirmed by SEM imaging of an aerogel made of sample B after 60 minutes of light irradiation (Figure 3g-h).

With this series of reference experiments in hands, we studied the possibility to freeze the supramolecular dynamic of the physical gel of sample B by permanent chemical cross-links in order to reinforce its mechanical properties. Reticulation of the physical network was performed via ROMP using Grubbs III catalyst. We initially probed the efficiency of the ROMP starting from solutions of compound **1**. At a concentration of 2 mM, either in toluene or dichloromethane, and using 0.3 equivalents of Grubbs III catalyst (i.e. 0.1 equivalent per norbornene unit),[24,29] only insoluble materials were recovered, thus suggesting full polymerization. By lowering the concentration to 0.05 mM in dichloromethane, we managed to obtain a solid which proved to be soluble in THF. While ^{1}H NMR and infra-red experiments confirmed the disappearance of the cyclo-olefinic double bond (Figure S6), GPC experiments suggested the formation of pentamers (see SI section 6). In the gel state, the polymerization was performed on either non-irradiated or light-irradiated sample B, at room temperature, and using 0.3 equivalents of Grubbs III catalyst. After an overnight reaction, methanol was used extensively to remove the catalyst and possibly remaining monomers from the cross-linked samples. The first evidence of the efficiency of the ROMP in the gel state was obtained by just manipulating the chemically cross-linked samples which appeared much more robust mechanically than its physical counterparts. The ROMP efficiency was further verified by a) infra-red spectroscopy which shows the disappearance of the band at 1335 cm^{-1} typical of the cyclo-olefinic double bond of norbornene (Figure S3b),[21] and b) thermogravimetric analysis (TGA) which clearly highlights the increased thermal robustness of the cross-linked samples (with a decomposition starting at 320°C) compared to the monomer (decomposition at 170°C) (Figure S7). The mechanical robustness of the cross-linked samples was then quantified by rheological experiments using a piezorheometer (Figure 4a-b).[30] In contrast to the previous measurements performed on physical gels, cross-linked gels were molded before performing shear measurements (see experimental section). For all the chemical gels studied, the storage modulus was found constant and the phase value close to zero, as expected for chemical gels in the low frequency regime.[31] Compared to the physical gel, storage moduli G' for non-irradiated and light-irradiated chemical gels are increased by ~2 orders of magnitude (G' = 22.5, 10.4 and 5.0 kPa for non-irradiated, 15 min and 60 min-irradiated chemical gels, respectively). Furthermore, the final rheological properties were similar whether the light irradiation occurred in the hot solution (before physical gelation) or directly in the physical gel state before chemical cross-linking by ROMP (Figure 4b). Therefore, the comparison of G' for the physical and the chemical gels,

with and without light irradiation, suggests that reticulation by chemical cross-links leads to the formation of thermodynamically stable polymer networks with an internal structure reminiscent of their physical counterparts. This structural interpretation by mechanical means was reinforced by cryo-SEM imaging of the non-irradiated chemical gel and by SEM imaging of xerogels arising from the covalently cross-linked irradiated gels. These micrographs indeed suggest very similar morphologies compared to the physical gels (Figure 4c-f). In addition, Medium and Wide Angle X-Ray scattering (MAXS and WAXS) experiments performed on these xerogels demonstrated the presence of a smectic-type packing as already observed for TATA-based supramolecular polymers,[5] which indicates that their main stacked organization is preserved in the cross-linked materials (Figure 4g). Analysis of the X-ray data indicates a pitch distance of ~28.4 Å and a N-N distance of 4.66 Å. These distances are very similar to the values recorded for the xerogel in toluene (27.8 Å and 4.72 Å, respectively) and to the initial values reported for supramolecular columns of TATA molecules (29.1 Å and 4.85 Å, respectively).[5] Altogether, these experiments indicate unambiguously that ROMP represents an efficient strategy to covalently capture triarylamine-based supramolecular polymers in order to further enhance their mechanical robustness while preserving their local structure.

We finally probed how the spectroscopic and conducting properties were affected by chemical cross-links. We observed that all chemical gels display increasing absorbance at ~820 and 1095 nm upon light irradiation; albeit with different intensities and kinetics depending on the way the corresponding physical gel was prepared (Figure 4h). On one hand, for the chemical gel prepared from a non-irradiated physical gel (Figure 4h, black data), we observed that light irradiation induces mainly an increase of the absorption band at ~820 nm, which corresponds to the presence of localized triarylammonium radicals. On the other hand, for the chemical gels prepared from light-irradiated physical gels (Figure 4h, red and blue data), light irradiation leads to a much larger increase of the absorption bands at 1095 nm, showing that these gels favor intermolecular through-space charge-transfer processes between stacked triarylamine cores. These observations also suggest that triarylamine units slightly change their ability to improve the radical delocalization upon light irradiation of the physical gel by improving their supramolecular stacks, a dynamic property which is apparently lost if the light irradiation is performed only after permanent cross-linking. The optical responses of the chemical gels can thus be modulated by the sample preparation and show a very interesting memory effect that combine dynamic structures and functions. We also evaluated the conductivity of the chemical gels upon light irradiation using a home-made ITO cell (Figure S8). However, the currents measured for all chemical gels were 4 orders of magnitude lower than those measured for the physical gels.

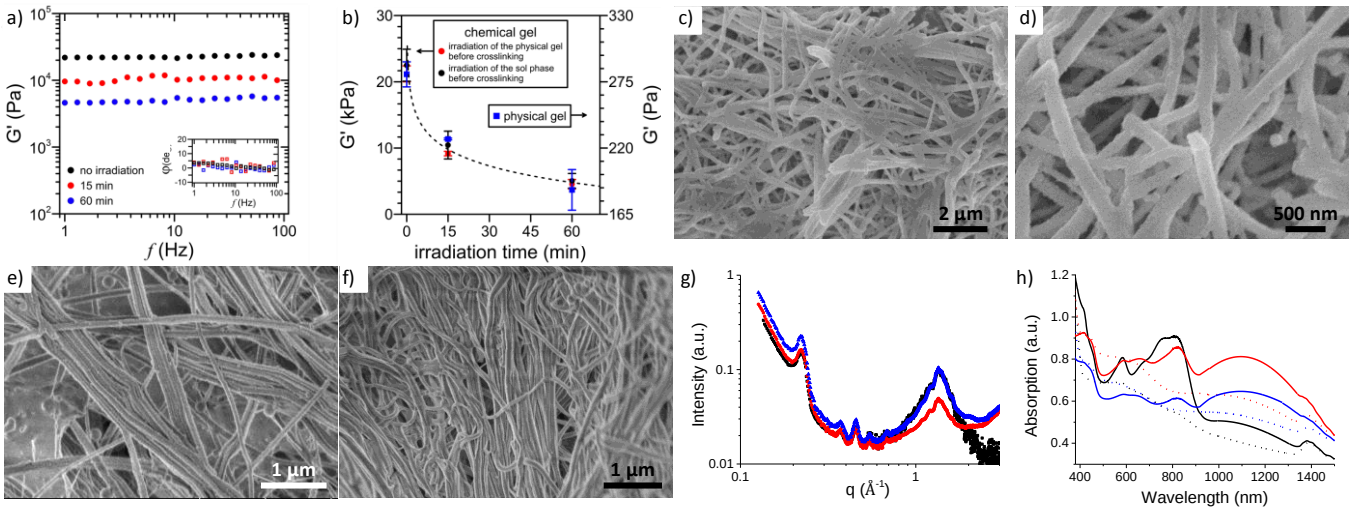

Figure 4. a) Variation of the storage modulus as a function of frequency for chemical gels made of **1** in a toluene/10% tetrachloroethane mixture: without light irradiation (black), with 15 minutes light irradiation (red), and with 60 minutes light irradiation (blue) in the gel phase. Experiments were recorded at 20°C. As it is the case or the physical gels, the phase of the chemical gel (in the insert) is roughly constant and independent of the light exposure time; b) Evolution of the storage modulus G' with irradiation times for physical gels (blue square), chemical gels irradiated in the gel phase before chemical cross-linking (red square), and chemical gels formed from an irradiated hot solution phase before cooling to the physical gel phase and subsequent chemical cross-linking (black dots). Experiments were recorded at 20°C. The dashed line is only a guide for the eyes. c-d) Cryo-SEM images of a chemical gel made of compound **1** in a toluene/10% tetrachloroethane mixture starting from a physical gel (15 mM, sample B) without irradiation; e-f) SEM images of the chemically cross-linked xerogel made of compound **1** in a toluene/10% tetrachloroethane mixture starting from a physical gel (15 mM, sample B) after 15 minutes (e) and 60 minutes (f) of light irradiation; g) MAXS-WAXS spectra of the chemically cross-linked aerogels made of compound **1** in a toluene/10% tetrachloroethane mixture starting from a physical gel (15 mM, sample B) without light irradiation (black), and with 15 minutes (red) and 60 minutes (blue) light irradiation in the gel phase; h) UV-Vis-NIR spectra of the chemical gel made of compound **1** in a toluene/10% tetrachloroethane mixture starting from a physical gel (15 mM, sample B) without light irradiation (black), and with 15 minutes (red) and 60 minutes (blue) of light irradiation in the gel phase. The dotted line spectra were recorded before further light irradiation of the chemical gels, whereas the plain line ones were recorded after further 60 minutes light irradiation of the chemical gels.

A tentative explanation for this difference rests on the fact that physical gels can easily recombine and rearrange their supramolecular structure in order to better contact their conducting core with the ITO surface. Such a dynamic being lost in the chemical gels, the charge injection and extraction in the active layer become more difficult to achieve. In addition, the crosslinking of the peripheral aliphatic chains also increases the resistance of the insulating layer around the TATA core, at both the interface with the electrodes and between the fibers, thus decreasing the overall conductivity of the material.

Conclusions

The present study shows the possibility to trap by covalent capture low molecular weight gelators involving triarylamine-based supramolecular polymers. To do so, ROMP is demonstrated as a particularly efficient method to freeze the fine supramolecular structure of the stacked TATA molecules and to significantly improve the mechanical properties of the corresponding chemical gel (i.e. with a typical gain of 2 orders of magnitude of the storage modulus). It should be noted that the use of ROMP directly in the physical gel state is novel in the literature, and this work highlights that the mild conditions used in the crosslinking procedure is of broad interest as potentially adaptable to other functional supramolecular systems. The physical properties of these systems are systematically studied in solution, in the physical gel, and in the chemical gel. Interestingly, it is shown that, by choosing the proper experimental conditions, the material can retain its main optical and local conducting properties – as for instance indicated by the presence of the NIR polaronic absorption band – when the phase transition occurs, and when the physical gel is subsequently and permanently reticulated. However, and although the internal conducting behaviour of the supramolecular fibers was retained after ROMP polymerization (as proved by the optical responses), the efficiency of the long-range conduction in the ITO device is significantly reduced for the chemical gel. This result can be explained by the loss of constitutional dynamics at the interface with the electrode and the higher resistance of the hydrophobic shell around the conducting TATA core after reticulation which limits the charge transport in the injection, extraction, and hopping processes. This result is however significant because it illustrates the general asset of supramolecular polymers – as for instance well illustrated to provide self-healing properties – by showing how their dynamics can be instrumental in improving some of their functional properties, including within devices. In addition, it challenges our imagination to enhance mechanical performances of soft functional materials. In that direction, a supramolecular polymerization directly performed within the device, and followed by covalent capture, emerges as a possible way of future investigations.

Experimental Section

General methods. All reactions were performed under an atmosphere of argon unless otherwise indicated. All reagents and solvents were purchased at the highest commercial quality and used without further purification unless otherwise noted. Dry solvents were obtained using a double column SolvTech purification system. Yields refer to purified spectroscopically (^{1}H NMR) homogeneous materials. Thin Layer Chromatographies were performed with TLC silica on aluminium foils (Silica Gel/UV254, Aldrich). In most cases, irradiation using a Bioblock VL-4C UV-Lamp (6 W, 254 nm and/or 365 nm) as well as phosphomolybdic acid and Cerium ammonium molybdate stainings were used for visualization. ESI-MS measurements were carried out on a Waters SQD apparatus. *^{1}H NMR spectra* were recorded on a Bruker Avance 400 spectrometer at 400 MHz and ^{13}C spectra at 100 MHz in $CDCl_3$ or CD_3CN at 25°C. The spectra were internally referenced to the residual proton solvent signal. For ^{1}H NMR assignments, the chemical shifts are given in ppm. Coupling constants *J* are listed in Hz. The following notation is used for the ^{1}H NMR spectral splitting patterns: singlet (s), doublet (d), triplet (t), multiplet (m), large (l). *UV-Vis-NIR spectra* were recorded on a Cary 5000 spectrophotometer using a quartz cuvette with 1.0 cm optical path length (for solutions), 1.0 mm optical path length (for physical gels) or a special cell for integration sphere measurements (chemical gels). *Infrared spectra* were recorded on a Fourier transform infrared spectrometer VERTEX 70 (Bruker) by drop-casting a solution or putting a small piece of dry gel sample on an ATR diamond probe. *Fluorescence emission spectra* were recorded on a FluoroMax-4 (Horiba) spectrofluorometer with the following settings: slit width = 5 nm, increment = 1 nm, integration time = 0.1 s in a quartz cuvette with a 1.0 cm optical path length. *EPR experiments* were recorded on a continuous-wave EPR X-band spectrometer (EMXplus from BrukerBiospin) equipped with a high sensitivity resonator (4119HS-W1, BrukerBiospin GmbH, Germany). Solutions samples were introduced into glass capillaries (Hirschm annrincap, 100 µL) and flame sealed prior introduction into 4 mm outer diameter quartz tubes. All gel samples were introduced directly into 4 mm outer diameter quartz tubes (Wilmad). Conventional field-swept spectra were performed during short intervals between stepwise illumination periods. The principal experimental parameters values were: a modulation amplitude of 1 G, a microwave power of ca. 2 mW, a time constant of ca. 40 ms, 120 ms conversion time and 200 G were swept in 120 s per scan and one scan was recorded after each illumination step. All experiments were performed at room temperature (295 K ± 1 K). *Rheological measurements* were carried out by using two different shear rheometers according to the nature of the gels: a conventional controlled-stress rheometer (Haake, Mars III) for physical gels and a home-made piezorheometer, i.e. working with piezoelectric elements, for chemical gels. Measurement in the chemical gels were performed after swelling. *AFM images* were obtained by scanning the samples using a Nanoscope 8 (Bruker) operated in Peak-Force tapping mode. Peak-Force AFM is based on Peak force tapping technology, during which the probe is oscillated in a similar fashion as it is in tapping mode, but at far below the resonance frequency. Each time the tip and the sample are brought together, a force curve is captured. These forces can be controlled at levels much lower than contact mode and even lower than tapping mode allowing operation on even the most delicate soft samples, as it is the case here. Ultra-sharp silicon tips on nitride lever were used (Bruker, Scanasyst with spring constant of 0.4 N/m). During AFM imaging, the force was reduced in order to avoid dragging of molecules by the tip. All analyses of the images were conducted in the integrated software. *TEM imaging* was performed using a CM12 Philips microscope equipped with a MVIII (Soft Imaging System) CCD camera. Samples were analyzed in Bright Field Mode with a LaB6 cathode and 120 kV tension. Image treatments were performed by using analySIS (Soft Imaging System) software. For the sample preparation, a piece of gel was dissolved in the swelling solvent then a 5 µL drop was cast on a grid that was placed on a Whatman paper. The grid was then left to dry under air before analysis. *SEM imaging* was performed on a FEG-SEM Hitachi SU8010 at room temperature at 1 kV. For xerogel and aerogel imaging, a small piece of gel was deposited on a silicon wafer covered with double sided tape. Before analysis, a piece of conductive tape was deposited on the wafer to ensure electrical contact between

the sample and the wafer. *CryoSEM:* To observe chemical gels in their native state, a small piece of gel was rapidly plunged into a nitrogen slush in the cryo preparation chamber of the Quorum PT 3010 machine. The frozen sample was then transferred under vacuum into the chamber attached to the microscope and fractured with a razor blade. Etching at -90 °C was performed followed by the deposition of a thin platinium layer. The sample is then transferred in the FEG-cryoSEM (Hitachi SU8010) and observed at -150 °C at 5 kV. *Conductivity experiments* were performed directly in commercially available transparent ITO electrode cells, with an active ITO area of 10x10mm, a 4 µm cell gap and no alignment layer (S100A040uNOPI LC cells from Instec, Inc.) for solutions and physical gel measurements. For experiments on chemically cross-linked gels, a home-made ITO cell was built from two glass substrates coated with ITO (Figure S8). Experiments were performed using a Keithley 2400 source meter with sweep cycles carried out below the electro-oxidation potential and ascend first.

Synthetic protocols. *Compound 1b:* A solution of compound **1a** (1.00 g, 2.87 mmol) and tin dichloride (7.22 g, 32.00 mmol) in a mixture of acetonitrile (40 mL) and ethanol (32 mL) was stirred overnight at 80 °C. After cooling down to room temperature, the solution was diluted with ethyl acetate (200 mL). The mixture was washed with $NaHCO_{3sat}$ (2 × 200 mL) and brine (150 mL). Then, the organic phase was dried over Na_2SO_4 and concentrated under reduced pressure to provide *N,N*-bis(4-aminophenyl)benzene-1,4-diamine, which was pure enough to be used as such in the next step. A solution of this crude compound and triethylamine (1.18 mL, 2.87 mmol) in dichloromethane (60 mL) was added dropwise to a cooled solution of 6-bromohexanoyl chloride (1.30 mL, 8.58 mmol) in dichloromethane (12 mL) at 0 °C under an argon atmosphere. The reaction mixture was heated up slowly to room temperature for 12 hours. Afterwards, solvents were removed under reduced pressure and the resulting crude residue was washed with dichloromethane several times (100 mL) to afford compound **1b** (920 mg, 39 %) as a white solid. ^{1}H NMR (CD_3OD:d_8-toluene 5:3, 400 MHz, 25°C): δ = 7.54 (d, ^3J = 8.8 Hz, 6H), 6.97 (d, ^3J = 8.8 Hz, 6H), 3.23 (t, ^3J = 6.8 Hz, 6H), 2.30 (t, ^3J = 7.4 Hz, 6H), 1.78-1.70 (m, 6H), 1.68-1.61 (m, 6H), 1.45-1.37 (m, 6H). ^{13}C NMR (CD_3OD:d_8-toluene 5:3, 100 MHz, 25°C): δ = 173.8, 145.3, 134.9, 125.2, 122.4, 37.7, 34.1, 33.6, 28.8, 26.0. ESI-MS: m/z calcd. for $C_{36}H_{45}Br_3N_4O_3$: 820.10 $[M]^+$, found: 820.15. These data are in agreement with data reported in the literature.[10]

Compound 1: An oven-dried flask was charged with 5-norbornene-2-carboxylic acid (0.20 mL, 1.647 mmol) and anhydrous potassium carbonate (0.68 g, 4.941 mmol) in dry dimethylformamide (15 mL). The reaction mixture was stirred at room temperature for 10 min and then, a solution of compound **1b** (150 mg, 0.183 mmol) and a catalytic amount of tetrabutylammonium iodide (20 mg, 0.054 mmol) in dimethylformamide (5 mL) was added. The solution was then stirred at room temperature for 6 hours. After that time, the solvent was evaporated under reduced pressure. The crude residue was dissolved in ethyl acetate (100 mL) and the organic phase was extracted with water (200 mL), brine (100 mL) and dried over Na_2SO_4. Further evaporation under reduced pressure and purification by column chromatography (SiO_2, cyclohexane → ethyl acetate/cyclohexane 3:2) provided compound **1** (90 mg, 50%) as a white solid. R_f = 0.3 (ethyl acetate /cyclohexane 3/2). ^{1}H NMR ($CDCl_3$, 400 MHz, 25°C): δ = 7.43 (s, 3H), 7.33 (d, ^3J = 8.4 Hz, 6H), 6.93 (d, ^3J = 8.4 Hz, 6H), 6.16 (dd, ^3J = 5.6, 3.1 Hz, 2H), 6.13 (dd, ^3J = 5.6, 2.9 Hz, 1H), 6.09 (dd, ^3J = 5.5, 3.0 Hz, 1H), 5.90 (dd, ^3J = 5.7, 2.8 Hz, 2H), 4.08 (t, ^3J = 6.7 Hz, 2H), 4.02 (dd, ^3J = 6.6, 3.1 Hz, 4H), 2.95-2.88 (m, 6H), 2.35 (t, ^3J = 7.4 Hz, 6H), 1.93-1.83 (m, 3H), 1.80-1.71 (m, 6H), 1.71-1.59 (m, 9H), 1.52-1.31 (m, 15H). ^{13}C NMR ($CDCl_3$, 100 MHz, 25°C): δ = 176.5, 175.0, 171.2, 138.2, 137.9, 135.9, 132.5, 64.1, 49.8, 46.8, 46.5, 45.9, 43.5, 43.4, 42.7, 41.8, 37.5, 30.5, 29.4, 28.6, 25.8, 25.4. ESI-MS: m/z calcd. for $C_{60}H_{72}N_4O_9$: 993.54 $[M+H]^+$, found: 993.68.

Preparation of physical and chemical gels. *Typical procedure for preparation of the physical gels*: Compound **1** (3.8 mg, 3.8 µmol) in either pure toluene (255 µL) or a 9:1 mixture of toluene/ tetrachloroethane (262 µL) was heated up to 90°C for 10 minutes and then cooled down to room temperature, leading to an homogeneous physical gel. Some of these gels were then lit in the gel phase.

Typical procedure for preparation of the chemical gels: In a vial, compound **1** (3.8 mg, 3.8 µmol) in a 9:1 mixture of toluene/ tetrachloroethane (262 µL) was heated up to 90°C for 10 minutes and then cooled down to room temperature, leading to an homogeneous mixture. After addition of a solution of Grubbs III catalyst (1.1 mg, 1.2 µmol) in toluene (127 µL), the mixture was shaken overnight at room temperature. Ethyl vinyl ether (0.38 mL) was added into the gel to quench the reaction and the vial was shaken for four hours. The resulting gel was washed several times with methanol (5 mL) and then methanol was exchanged with toluene by several washings. For light-irradiated samples, light irradiation using a 20W halogen lamp was performed in the gel state before addition of Grubbs catalyst.

Preparation of the chemical gels for rheological measurements: For the non-irradiated sample, in a vial, compound **1** (23.8 mg, 0.0238 mmol) in a mixture of toluene/tetrachloroethane (1.6 mL, 1.44/0.16 mL) was heated up to 90°C for 10 minutes and then introduced into a home-made mould (stainless steel, 2 mm thickness). After cooling down the mould to room temperature, a solution of Grubbs III catalyst (6.6 mg, 0.00727 mmol) in toluene (0.793 mL) was added. The mould was shaken overnight at room temperature. The formed gel was extracted from the mould and ethyl vinyl ether (2.4 mL) was allowed to diffuse into the gel to quench the reaction. After four hours, the resulting gel was washed several times with methanol (10 mL) and then methanol was exchanged with toluene by several washings.

For irradiated samples, in a vial, compound **1** (23.8 mg, 0.0238 mmol) in a mixture of toluene/tetrachloroethane (1.6 mL, 1.44/0.16 mL) was heated up to 90°C for 10 minutes and then cooled down to room temperature, leading to an homogeneous mixture. The mixture was exposed to light for 15 or 60 minutes, heated up (90°C) to become a clear solution and then introduced into the mould. Alternatively, light irradiation was also carried out in the solution phase at 90°C. Addition of Grubbs III catalyst and washing of the light-irradiated gels were performed following a protocol similar to the one described previously for the non-irradiated sample.

Acknowledgements

This work was supported by the Chinese Scholarship Council (CSC, fellowship to T. L.). We also wish to thank the CNRS, the Laboratory of Excellence for Complex System Chemistry (LabEx CSC), and the University of Strasbourg. The authors acknowledge Bertrand Vileno for EPR experiments, Guillaume Fleith for X-ray experiments, and "les plateformes d'analyse des polymères et de microscopie" from the Institut Charles Sadron.

Keywords: supramolecular polymers • triarylamines • gels • ROMP • rheology

[1] E. Moulin, J. J. Armao, N. Giuseppone, *Acc. Chem. Res.* **2019**, *52*, 975–983.
[2] I. Nyrkova, E. Moulin, J. J. Armao, M. Maaloum, B. Heinrich, M. Rawiso, F. Niess, J.-J. Cid, N. Jouault, E. Buhler, et al., *ACS Nano* **2014**, *8*, 10111–10124.
[3] E. Moulin, F. Niess, G. Fuks, N. Jouault, E. Buhler, N. Giuseppone, *Nanoscale* **2012**, *4*, 6748–6751.
[4] Y. Domoto, E. Busseron, M. Maaloum, E. Moulin, N. Giuseppone, *Chem. Eur. J.* **2015**, *21*, 1938–1948.
[5] J. J. Armao, M. Maaloum, T. Ellis, G. Fuks, M. Rawiso, E. Moulin, N. Giuseppone, *J. Am. Chem. Soc.* **2014**, *136*, 11382–11388.
[6] E. Busseron, J.-J. Cid, A. Wolf, G. Du, E. Moulin, G. Fuks, M. Maaloum, P. Polavarapu, A. Ruff, A.-K. Saur, et al., *ACS Nano* **2015**, *9*, 2760–2772.
[7] T. K. Ellis, M. Galerne, J. J. Armao, A. Osypenko, D. Martel, M. Maaloum, G. Fuks, O. Gavat, E. Moulin, N. Giuseppone, *Angew. Chem. Int. Ed.* **2018**, *57*, 15749–15753.
[8] A. Osypenko, E. Moulin, O. Gavat, G. Fuks, M. Maaloum, M. A. J. Koenis, W. J. Buma, N. Giuseppone, *Chem. Eur. J.* **2019**, DOI:10.1002/chem.201902898.
[9] V. Faramarzi, F. Niess, E. Moulin, M. Maaloum, J.-F. Dayen, J.-B. Beaufrand, S. Zanettini, B. Doudin, N. Giuseppone, *Nat. Chem.* **2012**, *4*, 485–490.
[10] J. J. Armao, Y. Domoto, T. Umehara, M. Maaloum, C. Contal, G. Fuks, E. Moulin, G. Decher, N. Javahiraly, N. Giuseppone, *ACS Nano* **2016**, *10*, 2082–2090.
[11] J. J. Armao, P. Rabu, E. Moulin, N. Giuseppone, *Nano Lett.* **2016**, *16*, 2800–2805.
[12] D. J. Cornwell, D. K. Smith, *Mater. Horizons* **2015**, *2*, 279–293.
[13] M. de Loos, J. van Esch, I. Stokroos, R. M. Kellogg, B. L. Feringa, *J. Am. Chem. Soc.* **1997**, *119*, 12675–12676.
[14] M. George, R. G. Weiss, *Chem. Mater.* **2003**, *15*, 2879–2888.
[15] D. D. Díaz, K. Rajagopal, E. Strable, J. Schneider, M. G. Finn, *J. Am. Chem. Soc.* **2006**, *128*, 6056–6057.
[16] M.-O. M. Piepenbrock, N. Clarke, J. A. Foster, J. W. Steed, *Chem. Commun.* **2011**, *47*, 2095–2097.
[17] C. S. Love, V. Chechik, D. K. Smith, I. Ashworth, C. Brennan, *Chem. Commun.* **2005**, 5647–5649.
[18] J. R. Moffat, I. A. Coates, F. J. Leng, D. K. Smith, *Langmuir* **2009**, *25*, 8786–8793.
[19] I. A. Coates, D. K. Smith, *Chem. Eur. J.* **2009**, *15*, 6340–6344.
[20] E. Bellmann, S. E. Shaheen, S. Thayumanavan, S. Barlow, R. H. Grubbs, S. R. Marder, B. Kippelen, N. Peyghambarian, *Chem. Mater.* **1998**, *10*, 1668–1676.
[21] T. Yamamoto, T. Fukushima, Y. Yamamoto, A. Kosaka, W. Jin, N. Ishii, T. Aida, *J. Am. Chem. Soc.* **2006**, *128*, 14337–14340.
[22] T. Yamamoto, T. Fukushima, A. Kosaka, W. Jin, Y. Yamamoto, N. Ishii, T. Aida, *Angew. Chem. Int. Ed.* **2008**, *47*, 1672–1675.
[23] T.-Y. Luh, *Acc. Chem. Res.* **2013**, *46*, 378–389.
[24] K.-W. Yang, J. Xu, C.-H. Chen, H.-H. Huang, T. J.-Y. Yu, T.-S. Lim, C. Chen, T.-Y. Luh, *Macromolecules* **2010**, *43*, 5188–5194.
[25] E. Moulin, F. Niess, M. Maaloum, E. Buhler, I. Nyrkova, N. Giuseppone, *Angew. Chem. Int. Ed.* **2010**, *49*, 6974–6978.
[26] B. Adelizzi, I. A. W. Filot, A. R. A. Palmans, E. W. Meijer, *Chem. Eur. J.* **2017**, *23*, 6103–6110.
[27] K. Y. Kim, C. Kim, Y. Choi, S. H. Jung, J. H. Kim, J. H. Jung, *Chem. Eur. J.* **2018**, *24*, 11763–11770.
[28] K. Lancaster, S. A. Odom, S. C. Jones, S. Thayumanavan, S. R. Marder, J.-L. Brédas, V. Coropceanu, S. Barlow, *J. Am. Chem. Soc.* **2009**, *131*, 1717–1723.
[29] T.-L. Choi, R. H. Grubbs, *Angew. Chem. Int. Ed.* **2003**, *42*, 1743–1746.
[30] J.-R. Colard-Itté, Q. Li, D. Collin, G. Mariani, G. Fuks, E. Moulin, E. Buhler, N. Giuseppone, *Nanoscale* **2019**, *11*, 5197–5202.
[31] M. Rubinstein, R. H. Colby, *Polymer Physics*, Oxford University Press, Oxford, New York, **2003**